Appl. Phys. B (2012) 109:573–579
DOI 10.1007/s00340-012-5156-9

Applied Physics B
Lasers and Optics

Poling pattern for efficient frequency doubling of Gaussian beams

Roy Shiloh · Ady Arie

Received: 31 July 2011 / Revised: 29 April 2012 / Published online: 15 September 2012

Abstract The commonly used periodic patterning for quasi phase-matching plane-waves is theoretically adequate for completely depleting and transferring a fundamental wave to its second harmonic. However, when working with Gaussian beams the conversion efficiency of such a design lacks due to the inherent Gouy phase shift and the spatially varying beam profile, yielding roughly 88 % conversion efficiency. In this paper, we study the possibility of adding a linear chirp and Gouy-phase shift compensation to the periodic poling. We demonstrate that this poling pattern enables us to achieve near-optimal frequency doubling efficiency of up to 97 %.

1 Introduction

When designing a periodically poled crystal to frequency-double an input fundamental plane-wave, the period can simply be deduced from the quasi phase-matching (QPM) condition. This method allows one to theoretically achieve the optimal efficiency, fully converting the fundamental wave to its second harmonic (SH). Efficient generation of higher harmonics of a plane-wave pump is also possible using a numerical optimization algorithm [1]. Considering the practical case of a Gaussian beam, however, a periodic design will not yield perfect conversion. The inherent Gouy phase creates an additional phase factor, dependent on the longitudinal coordinate, which is not compensated for by the periodic design. Previous studies have dealt with the Gouy phase-shift [2, 3], and the inherent Gaussian wave phase mismatch has been discussed, but these studies did not take pump depletion into account. In addition, since the conversion efficiency curve varies with intensity, the Gaussian intensity profile will not convert equally, and partial back-conversion may occur. Boyd and Kleinman [4] have addressed this issue, but only in the undepleted pump approximation. It was shown that for the case of third harmonic generation of a Gaussian fundamental beam, near-optimal efficiency is possible [5], but an optimal pattern for frequency doubling of a Gaussian beam has not been found yet. In this article we propose a design that compensates for the Gouy phase-shift and the Gaussian profile and show that such a design can convert 97 % of the energy of a fundamental Gaussian beam into the SH wave. The article is arranged as follows: in Sect. 2 we describe the phase-mismatch due to the Gaussian nature of the beam and theoretically derive appropriate corrections. In Sect. 3, we analyze the proposed corrections in a numerical simulation. In Sect. 4, experimental results are provided and compared to theory. We summarize in Sect. 5.

R. Shiloh (✉) · A. Arie
Department of Physical Electronics,
School of Electrical Engineering,
Fleishman Faculty of Engineering, Tel Aviv University,
69978 Tel Aviv, Israel
e-mail: royshilo@post.tau.ac.il

2 Deriving the phase-mismatch correction term

We define the complex amplitude of the Gaussian field as follows [6]:

$$E(r,z) = \frac{A(z)}{1+i\zeta} e^{-r^2/\omega_0^2(1+i\zeta)} \quad (1)$$

where $A(z)$ is the field amplitude, r the spatial profile coordinate, ω_0 the beam waist and ζ is a dimensionless longitudinal coordinate defined in terms of the confocal parameter b

$$\zeta = 2z/b = 2z/k\omega_0^2 \tag{2}$$

The Gaussian phase is comprised of two factors: the Gouy phase shift atan(ζ) due to the factor in the denominator, $1 + i\zeta$, and an additional phase factor in the transverse direction, of the form $\propto r^2 \cdot \zeta/(1 + \zeta^2)$, that arises from the spatial nature of the Gaussian beam. The total phase therefore consists of these two factors and the spatial harmonic phase, exp(ikz).

Applying QPM, we suggest compensating the phase-mismatch by modulating the effective nonlinear coefficient in the following general form:

$$d(z) = d_{\text{eff}} \cdot \text{sign}\{\ \cos[\beta(z) - \text{atan}(\zeta)]\} \tag{3}$$

where atan(ζ) compensates for the Gouy phase shift and $\beta(z)$ corrects the spatial profile along the propagation length. We expand $\beta(z) = \beta_0 + \beta_1 \cdot z + \beta_2 \cdot z^2 + \cdots$: β_0 is a constant phase factor and may be ignored; $\beta_1 \cdot z$ is theoretically optimized as $\Delta k \cdot z$, where $\Delta k = k_{2\omega} - 2\ k_{\omega}$ is the phase mismatch between the interacting waves. Boyd and Kleinman [4] showed that the optimal phase mismatch for a Gaussian beam depends on the focusing parameter l/b where l is the optical length and b is the confocal parameter and in general is not zero, so one may argue that a slightly different value is required for β_1. However, the derivation in [4] assumed that the pump is not depleted and that the phase-matching pattern is not a function of the longitudinal coordinate. By numerical simulations, we found that even when the pump is strongly depleted, the optimal choice for β_1 is Δk.

The quadratic term $\beta_2 \cdot z^2$ provides a linear chirp to the period. Chirped patterns have previously been demonstrated to show beneficial qualities in sum-frequency conversion [7]. In our case, this term contributes another degree of freedom for compensating the spatial beam variations as it propagates. It is therefore concluded that for second order polynomial expansion of $\beta(z)$, the poling pattern is dependent only on one parameter, β_2:

$$d(z) = d_{\text{eff}} \cdot \text{sign}\{\cos[\Delta k \cdot z + \beta_2 \cdot z^2 - \text{atan}(\zeta)]\} \tag{4}$$

In order to investigate the effect of the correction parameter β_2 for compensating the transverse Gaussian phase factor, we define the local phase-mismatch function $f(r, z)$, which is the difference between the correction

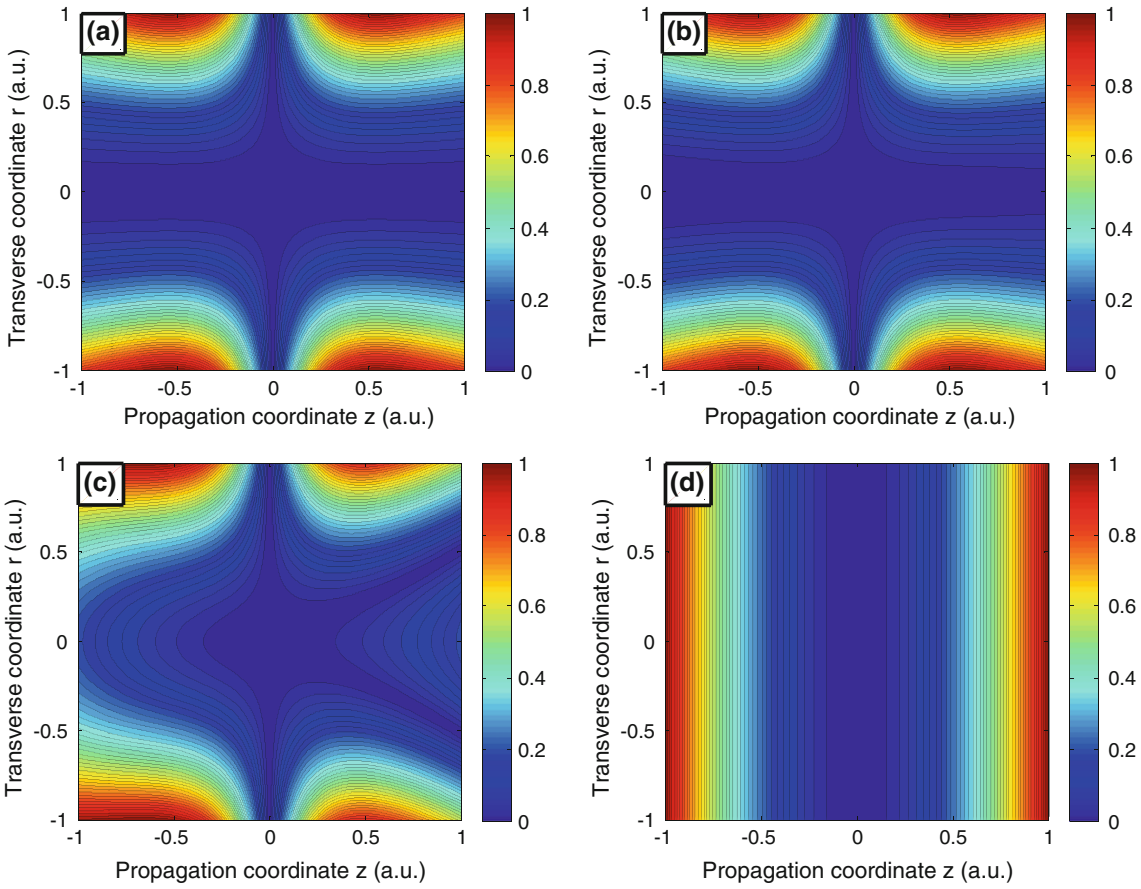

Fig. 1 Qualitative depiction $|f(r, z)|$, indicating local phase-mismatch, in normalized units, of the angular spread of k-vectors in a focused Gaussian beam as it propagates in a periodic (**a**), negative (**b**) and positive (**c**) β_2 design. *Darker areas* (*blue*) are where the phase-mismatch is minimal. (**d**) Example of phase-matching if β_2 is chosen too large, or if the Gaussian wave is replaced with a plane-wave

parameter and the Gaussian phase factor, $f(r, z) = \pm(r^2/\omega_{0,\mathrm{eq}}^2) \cdot \zeta/(1+\zeta^2) + \beta_2 \cdot z^2$. $\omega_{0,\mathrm{eq}}^2 = \omega_{0,1}^2 \cdot \omega_{0,2}^2/(\omega_{0,1}^2 - 2\omega_{0,2}^2)$ is a constant, which results when substituting Eq. (1) as the interacting field in the SH coupled-wave equations [6], where $\omega_{0,1}^2$, $\omega_{0,2}^2$ are the fundamental and SH beam waists, respectively. Figure 1 qualitatively illustrates $|f(r, z)|$ for several values of β_2, specifically zero and optimized negative and positive values—we have numerically found that two distinct peak efficiencies exist depending on the sign of β_2. Note that minimal phase-mismatch is obtained where $f(r, z) \to 0$ (darkest blue in the figure).

Figure 1a is a periodic design, $\beta_2 = 0$, and as the beam focuses ($z = 0$) all k-vectors are parallel and thus are efficiently phase-matched. Away from the focus, only k-vectors parallel to the propagation axis ($r = 0$) have the least phase-mismatch. In Fig. 1b, β_2 is negative and small; it is noticeable that the diagram is similar to the periodic case but slightly asymmetric: at $z \ll 0$, k-vectors with a larger angle to the propagation axis are more efficiently phase-matched and this slight difference will later be shown to have a strong impact on conversion efficiency. In Fig. 1c β_2 is positive and relatively large; in this design, up until the focal point where the bulk of the conversion is done, we observe a gradual improvement in the phase-matching efficiency, and beyond it only specific k-vectors with large transverse components are efficiently phase-matched. The optimal positive β_2 would be one that phase-matches most k-vectors around the center of the crystal ($z = 0$), and allow a longer interaction length for those that propagate off-axis ($r \neq 0$), and thus diffract strongly. Figure 1d shows, as reference, an example of a plane-wave or alternatively a large, non-optimal choice of β_2 (where the most efficient conversion is around $z = 0$, so the effect of β_2 is weak).

We finish describing the effect of $\beta_2 \cdot z^2$ by recalling that the beam intensity has a Gaussian profile and that the nonlinear process is quadratically dependent on the local fundamental amplitude. We would like to design a poling pattern that compensates for this by allowing a proportionally longer interaction length for the lower-intensity tails of the Gaussian, and a shorter interaction length for the central, intensity-wise powerful peak; it is possible to distinguish in QPM between the tails and the central peak because any part of the beam, which is off-axis and far from the beam waist has an angular spread of k-vectors, to which we can design appropriate QPM patterns. Observing Fig. 1b and c, our choice has done just that; as the beam propagates, selected k-vectors are depleted (they convert to the SH), and so a continuous change in the phase-matching condition allows us to phase-match different k-vectors and give more weight to the ones farther from the theoretical plane-wave phase-matching condition.

3 Numerical simulations

In this section, based on chosen material and equipment parameters, we separately find positive and negative optimal (highest efficiency) values for β_2. We then present simulations with the waists giving peak efficiency as a function of propagation length, input power and temperature. We conclude by discussing the results.

Using the split-step Fourier method [8], we have chosen to simulate a KTP crystal at 100 °C and an input Gaussian wave of wavelength 1,064.5 nm and 2 kW peak power, representing a continuous-wave or flat-top pulse. For the positive β_2 we have chosen a crystal of length 25 mm, and for the negative β_2 a length of 12.5 mm. We then scanned over a wide range of beam waists, from 10 to 150 μm (see Fig. 2), and chose the most efficient. The algorithm designed to find β_2 is based on the golden section search method [9]. We chose a longitudinal step resolution of 0.1 μm. The simulation was conducted over a transverse

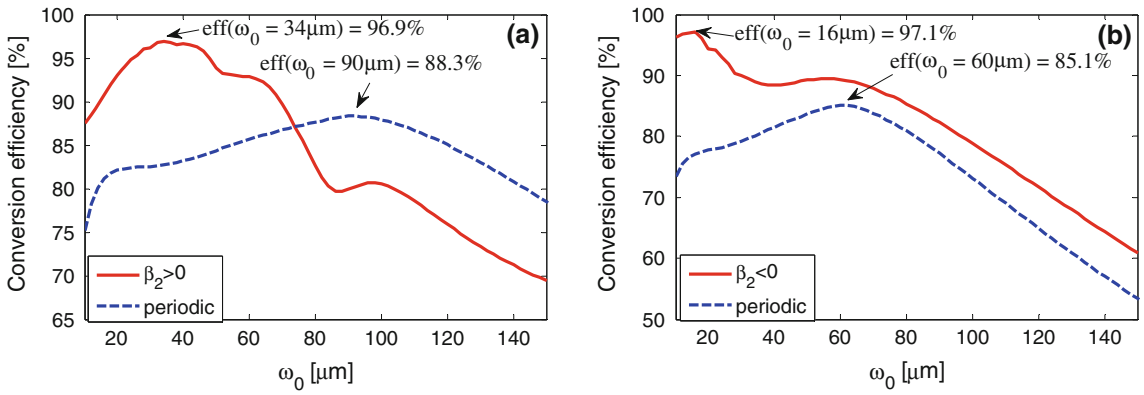

Fig. 2 Beam waist tuning for optimal efficiency. **a** *Line* (*red*) and *dashed* (*blue*)—positive $\beta_2 = 793.16\ \mathrm{m}^{-2}$ and corresponding periodic pattern; crystal length is 18.54 mm. **b** *Line* (*red*) and *dashed* (*blue*)—negative $\beta_2 = -11.3\ \mathrm{m}^{-2}$ and corresponding periodic pattern; crystal length is 10.85 mm

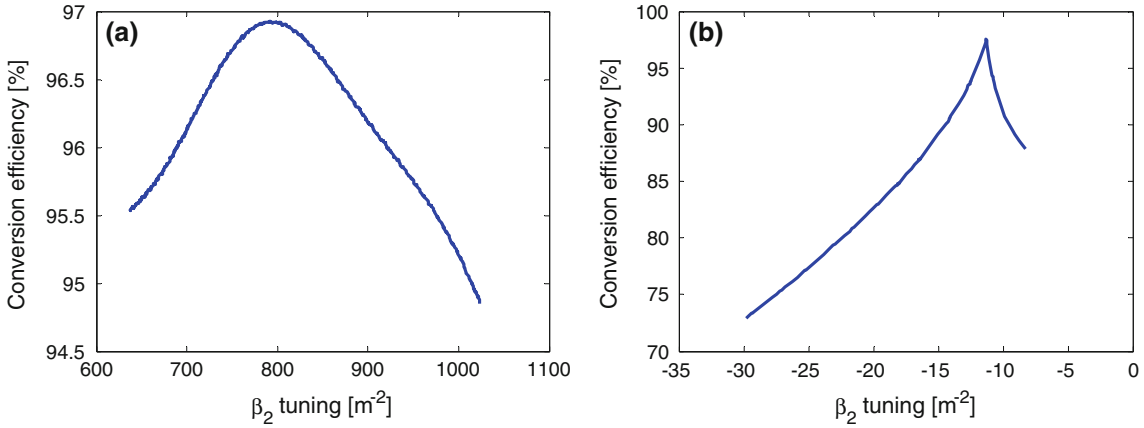

Fig. 3 Tuning curves for positive (**a**) and negative (**b**) β_2. **a** A positive value of $\beta_2 = 793.16\ \mathrm{m}^{-2}$ is found for $\omega_0 = 34\ \mu\mathrm{m}$ and crystal length of 25 mm. **b** A negative value of $\beta_2 = -11.3\ \mathrm{m}^{-2}$ is found for $\omega_0 = 16\ \mu\mathrm{m}$ and crystal length of 12.5 mm

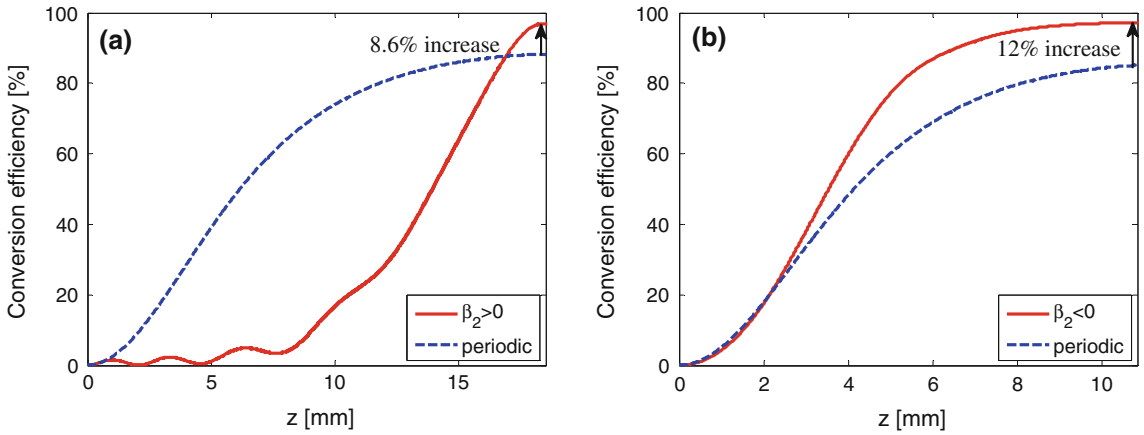

Fig. 4 **a** SH propagation plots for positive $\beta_2 = 793.16\ \mathrm{m}^{-2}$ and the corresponding periodic pattern with waist 34 and 90 μm, respectively. Crystal length is 18.54 mm. **b** SH propagation plots of negative $\beta_2 = -11.3\ \mathrm{m}^{-2}$ and the corresponding periodic pattern with waist 16 and 60 μm, respectively. Crystal length is 10.85 mm

area, which was about five times larger than the input beam radius in each one of the two transverse coordinates. Each cell's dimension in the simulation matrix is one-tenth the beam waist; these parameters were found to give a negligible amount of numerical errors.

The peak efficiency is not necessarily reached at the crystal's end facet, thus we truncate the crystal appropriately to avoid back-conversion. For positive and negative β_2, the optimal waist is 34 μm at $\beta_2 = 793.16\ \mathrm{m}^{-2}$ and 16 μm at $\beta_2 = -11.3\ \mathrm{m}^{-2}$ (yielding an intensity of 110 and 500 MW/cm^2), respectively. The β_2 tuning curves for these waists are shown in Fig. 3. It is observed that the positive β_2 tuning curve is much broader than the negative β_2 one; around the peak value, the positive β_2 may vary as much as 120 m^{-2} for a change of 1 % in efficiency, while variation as little as 0.105 m^{-2} incurs 1 % efficiency change for the negative β_2. For comparison, in the case of the periodic pattern we chose optimal beam waists of 60 and 90 μm, for crystal lengths of 10.85 and 18.54 mm, respectively. Results as a function of propagation length are depicted in Fig. 4a and b.

It is evident from the simulations that both the positive and negative β_2 designs provide higher conversion efficiency with respect to the periodic pattern. In case of positive (negative) β_2 the higher conversion efficiency is 96.9 (97.1) % as opposed to a conversion efficiency of 88.3 (85.1) % in the periodic pattern, thereby representing an improvement of 8.6 (12) % in conversion efficiency.

The dependence of the conversion efficiency and temperature acceptance on the input power is shown in Fig. 5. The positive β_2 results in a weaker conversion efficiency for lower input powers but reaches higher efficiencies otherwise in Fig. 5a. The negative β_2 shows a distinct improvement over the corresponding periodic pattern in Fig. 5c. The temperature acceptances, shown in Fig. 5a and d, are broadest for the positive β_2 design, which allows for

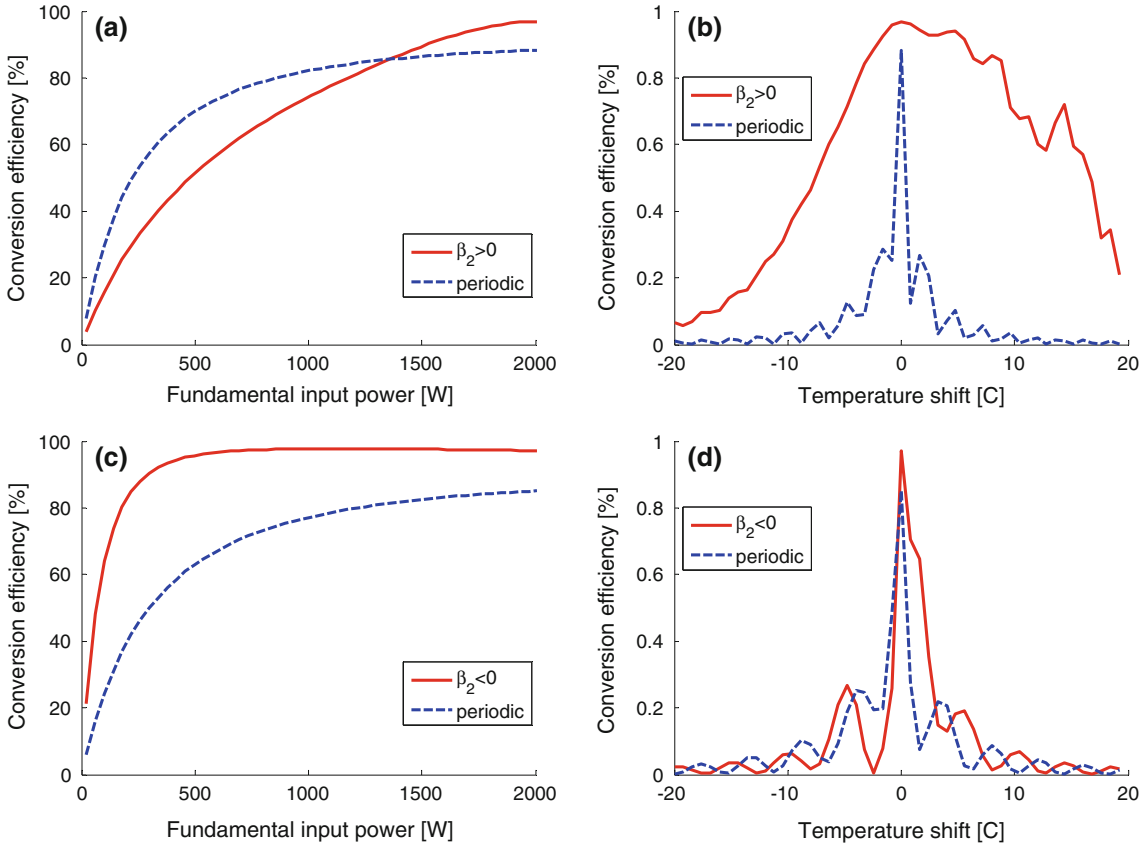

Fig. 5 **a**, **c** Conversion efficiency curves for positive β_2 and negative β_2, and their corresponding periodic patterns, respectively. **b**, **d** The related temperature acceptance curves

Table 1 Summary of pulse-conversion efficiencies

Design	Optimal waist (μm)	Crystal length (mm)	Flat-top pulse efficiency (%)	Gaussian pulse efficiency (%)	Numerical value of β_2 (m^{-2})
Positive β_2	34	18.54	96.9	82.2	793.16
Periodic	90	18.54	88.3	81.6	–
Negative β_2	16	10.85	97.1	93.1	−11.3
Periodic	60	10.85	85.1	77.6	–

good conversion efficiency in temperature-wise unstable environments.

The conversion efficiency curves can serve as a basis for predicting the conversion efficiencies of long pulses other than flat-top, for example, Gaussian pulses, or for pulse shaping applications. This interpretation may be explained mathematically by first finding the function $P_{\text{out}} = g(P_{\text{in}})$ that describes the conversion curve (for example, the red curve in Fig. 5c multiplied by P_{in}); for each input power P_{in}, the conversion efficiency is given by g/P_{in}. Therefore, for an arbitrary input pulse, the total conversion efficiency η is deduced from the relation $\eta = \int g(P_{\text{in}}(\tau))\mathrm{d}\tau / \int P_{\text{in}}(\tau)\mathrm{d}\tau$. Table 1 summarizes results for flat-top (or quasi-monochromatic) and Gaussian pulses sharing the same peak power of 2 kW.

4 Experimental results and conclusions

We used the electric field poling technique in order to modulate the nonlinear coefficient of a KTP crystal. The accepted damage threshold for KTP is about 500 MW/cm^2 for 10 ns pulses (http://www.as.northropgrumman.com/products/synoptics_ktp/assets/ktp.pdf), and to avoid it we decided to design our experiment for a 25 μm beam waist for which, assuming peak power of 2 kW, the intensity is roughly 200 MW/cm^2. We manufactured three different designs: having positive β_2, negative β_2 and a periodic pattern for comparison, each of which with an underlying phase-matching period of 8.85 μm. The quasi-monochromatic, 5 ns-pulsed laser outputted a Gaussian beam centered at 1.064 μm at a repetition rate of 10 kHz and peak power of 2 kW. As in Sect. 3, after finding the optimal β_2 values for the chosen beam waist, the designs were truncated at the correct length for optimal conversion efficiency. The expected and measured temperature acceptances are summarized in Table 2, along with the

optimal values of β_2. The measured temperature acceptance is depicted in Fig. 6. We have made several attempts at measuring the different designs, but the results, aside from the temperature acceptance of the positive β_2 design, which agrees well with theory, were unsatisfactory. The setup included a spatial filtering section consisting of two pinholes and lens in a telescope formation to achieve beam quality $M^2 = 1 \pm 0.1$ and a 50–50 beam-splitter with two photodiode detectors to measure the crystal input and output simultaneously.

It is observed that we could not exactly follow the simulated temperature acceptance, the experimental curves smoother in comparison to the simulated ones. Our measurements were strongly affected by the laser's output power, which showed strong fluctuations over short periods of time, sometimes damaging the crystal. The temperature gradient in the crystal and the instability and inaccuracy of the oven further hampered our attempts. Lastly, each pulse varied greatly in amplitude and slightly in form, complicating the treatment of the results. We believe that for these reasons we could not achieve our theoretical goals, and the efficiency measurements were not accurate enough. It is worth mentioning that the expected sinc function [6] for the temperature acceptance of a periodic pattern is not observed in the simulation since we are employing a focused Gaussian beam rather than an undepleted-pump plane-wave.

Table 2 Summary of expected efficiencies for 25 μm waist

Design	Channel length (mm)	Flat-top pulse efficiency (%)	Gaussian pulse efficiency (%)	Numerical value of β_2 (m^{-2})
Positive β_2	16.78	95.2	82.5	745.84
Negative β_2	11.16	91.9	87.0	−37.01
Periodic	10.10	84.2	77.2	–

5 Summary

In this article, we suggested a method tailored to phase-match a Gaussian beam with a 1D pattern. The method offers a theoretical improvement of up to 12 % for flat-top pulses at 2 kW and up to 15.5 % for Gaussian pulses, over the plane-wave periodic pattern solution. We have run numerical simulations on KTP and considered practical

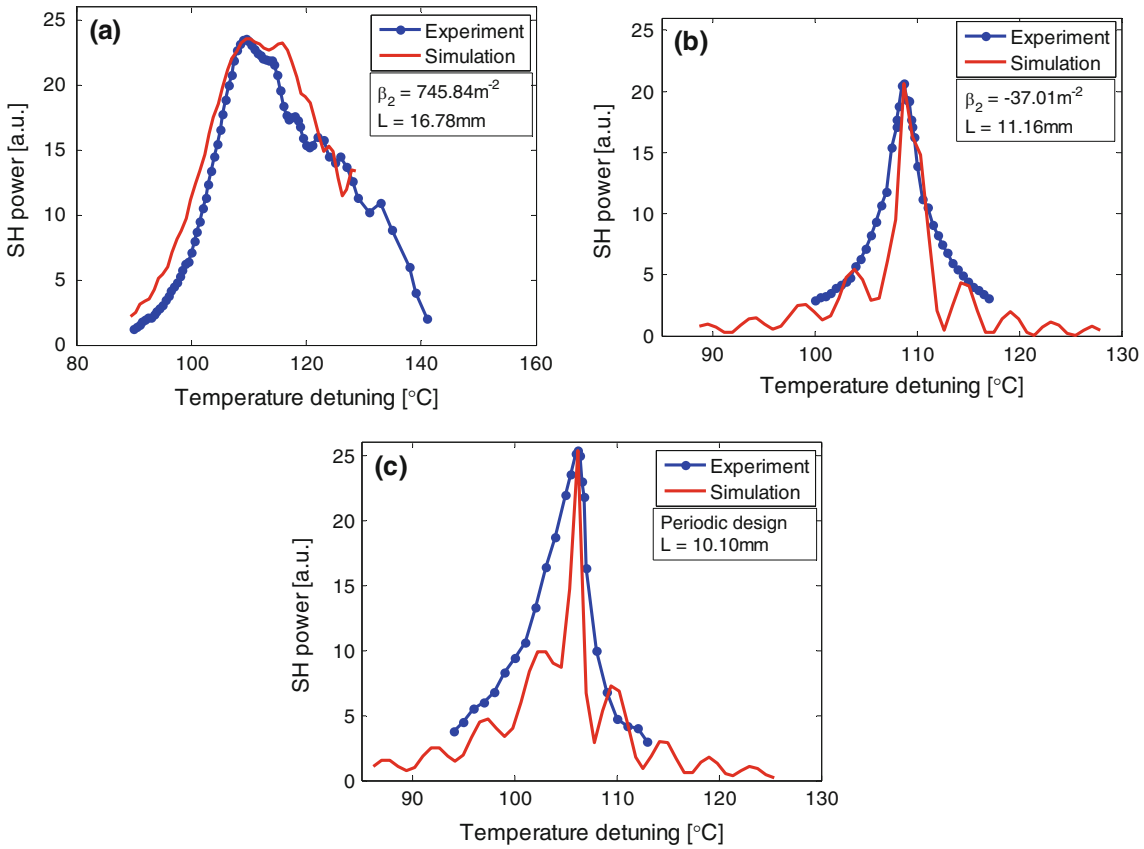

Fig. 6 Measured and normalized theoretical curves of temperature acceptances for each channel. Theoretical (*red*) and measured (*blue*) data for **a** positive β_2, **b** negative β_2, **c** periodic pattern

aspects such as beam intensity and temperature acceptance. We fabricated a crystal with the different designs. Measurements have shown that the temperature acceptance of the crystals fit well the theoretical predictions. Conversion efficiency measurements were also performed but the calculated improvement could not be observed clearly due to non-ideal measuring conditions. The method may be applied to other nonlinear optics crystals by finding the chirp parameter β_2, which brings the conversion efficiency to a maximum.

Acknowledgments This work was partially supported by the Office of the Chief Scientist, The Israeli Ministry of Industry, Trade and Labor.

References

1. U.K. Sapaev, G. Assanto, Opt. Express **16**, 1 (2008)
2. H.E. Major, C.B.E. Gawidth, P.G.R. Smith, Opt. Commun. **281**, 5036–5040 (2008)
3. N. Lastzka, R. Schanbel, Opt. Express **15**(12), 7211 (2007)
4. G.D. Boyd, D.A. Kleinman, JOAP **39**(8), 3597 (1968)
5. C. Zhang, Y. Qin, Y. Zhu, Opt. Lett. **33**(7), 720–722 (2008)
6. R.W. Boyd, *Nonlinear Optics* (Academic Press, New York, 2008)
7. H. Suchowski, V. Prabhudesai, D. Oron, A. Arie, Y. Silberberg, Opt. Express **17**(15), 12731–12740 (2009)
8. G.P. Agrawal, *Nonlinear Fiber Optics* (Academic Press, Boston, 1995)
9. W.H. Press, S.A. Teukolsky, W.T. Vetterling, B.P. Flannery, *Numerical Recipes in C: The Art of Scientific Computing* (Cambridge University Press, London, 1992)